E2-2003-164

D. V. Bandurin[1], N. B. Skachkov[2]

ON THE POSSIBILITY OF MEASURING THE GLUON DISTRIBUTION IN PROTON WITH «γ + jet» EVENTS AT **LHC**

Submitted to «European Physical Journal C»

[1]E-mail: dvm@cv.jinr.ru
[2]E-mail: skachkov@cv.jinr.ru

1. Introduction

The modeling of the production processes of many new particles (Higgs boson, SUSY particles) in the forthcoming LHC experiments as well as future physical analysis of corresponding measurement are heavily based on the knowledge of gluon distribution in a proton $f_g^p(x, Q^2)$ [1] [1]. For this reason the study of the possibility of the measuring gluon density directly in the LHC experiments (especially in the kinematic region of small x and high Q^2) is of a big interest.

One of the promising channels for this measurement is an inclusive prompt photon production [2]

$$pp \to \gamma^{dir} + X. \tag{1}$$

The region of photon transverse momentum P_t^γ, reached by UA1 [3], UA2 [4], CDF [5] and D0 [6] experiments, extends up to $P_t^\gamma \approx 60\ GeV/c$ and, according to recent results [7], up to $P_t^\gamma \approx 105\ GeV/c$. These data together with the later ones (see references in [8]–[19]) and E706 [20], UA6 [21] results give, in principle, an opportunity for tuning the form of gluon distribution (see [13, 16, 22, 23]). The rates and an estimation for cross sections of inclusive photon production at LHC are given in [2] (see also [24]).

Here we consider the process of a direct photon production in association with an opposite-side jet [12, 13] (for experimental results see [25, 26, 27])

$$pp \to \gamma^{dir} + jet + X. \tag{2}$$

In QCD leading order the processes (1) and (2) are caused by two subprocesses: the "Compton-like" scattering

$$qg \to q + \gamma \tag{3}$$

and the "annihilation" subprocess [2]

$$q\overline{q} \to g + \gamma. \tag{4}$$

The first one gives a dominant contribution to the cross sections of (1) and (2) [8, 12, 13] and serves as "signal" subprocess due to its direct connection with the gluon distribution.

The study of "$\gamma + jet$" process (2) is a more preferable as compared with the inclusive direct photon production process (1) from the viewpoint of extraction of information on the gluon distribution $f_g^p(x, Q^2)$ [3]. First of all, it is explained by a higher

[1] For example, the production of Standard Model Higgs boson is mainly caused by gluon-gluon fusion $gg \to H$ over the entire mass range [1].

[2] A contribution of another possible NLO channel $gg \to g\gamma$ was found to be still negligible even at LHC energies.

[3] A detailed study of "$\gamma + jet$" events and different aspects of their application can be found in [28, 29].

value of a purity of the process (2), for which the signal-to-background (S/B) ratios are several times higher than S/B ratios to process (1) [31, 32]. Secondly, while the cross section for the process (1) is given as an integral over the parton distribution functions (PDF) of a proton $f_a^p(x, Q^2)$, the cross section of the process (2) is expressed directly (at $P_t{}^\gamma \geq 30/\ GeV/c$ [4]) through these PDFs:

$$\frac{d\sigma}{d\eta_1 d\eta_2 d(P_t^\gamma)^2} = \sum_{a,b} x_a\, f_a^p(x_a, Q^2)\, x_b\, f_b^p(x_b, Q^2) \frac{d\sigma}{d\hat{t}}(a\, b \to 1\, 2), \qquad (5)$$

where $a, b = q, \bar{q}, g$; $1, 2 = q, \bar{q}, g, \gamma$. The incident parton momentum fractions x_a, x_b may be reconstructed from the final state photon and jet pseudorapidities $\eta_1 = \eta^\gamma$, $\eta_2 = \eta^{jet}$ and $P_t{}^\gamma$ according to formula [5]

$$x_{a,b} = P_t{}^\gamma/\sqrt{s} \cdot (exp(\pm\eta_1) + exp(\pm\eta_2)). \qquad (6)$$

Thus, formula (5) with the knowledge of the experimentally determined triple cross section in the intervals of $\Delta\eta^\gamma$, $\Delta\eta^{jet}$ and $(P_t^\gamma)^2$ and with account of results of independent measurements of q, $\bar{q}$ distributions [33] allows the gluon distribution $f_g^p(x, Q^2)$ to be determined after essential reduction of a background contribution.

The $P_t{}^\gamma$ distributions of the number of signal events remained after application of strict selection criteria, proposed in [31, 34], were presented earlier in [29, 30, 35, 36] [6]. Those selection criteria allow to reduce considerably the background to "$\gamma^{dir} + jet$" process (2) and select the events with a suppressed initial state radiation. Here we present the detailed study of background fraction in different x- and Q^2-intervals and show that "gluonic" subprocess (3) gives a noticeable contribution [30].

This paper is organized as follows. The main background sources are discussed in section 2. In section 3 we list the selection criteria used to enhance the content of the signal events (3) in the selected data sample. In section 4 the numbers of the events suitable for an extraction of the gluon distribution function $f_g^p(x, Q^2)$ are estimated. The contribution of events of other types in different x- and Q^2- intervals are also shown in this section. A possibility of the further background events suppression by an account of the discrimination efficiencies between a single photon and π^0, η, ω and K_s^0 mesons as well as between quark and gluon jets is also demonstrated.

2. Background sources

The background to the events based on the process (2) is mainly caused by:

— the events with high P_t photons produced in the neutral decay channels of π^0, η, ω and K_s^0 mesons [7].

[4] i.e. in the region where "k_T smearing effects" should not be important (for example, see [18]).

[5] see, for instance, [11, 12].

[6] Analogous estimations for the Tevatron were done in [37, 38].

[7] As it was shown in [39] the charged decay channels of those mesons can be strongly suppressed even without a tracker information.

— the events with the photons radiated from a quark (i.e. bremsstrahlung photons) in the next-to-leading order QCD subprocesses of the $qg \to qg$, $qq \to qq$ and $q\bar{q} \to q\bar{q}$ scattering [31, 32].

The background events of the first type will be called below as the "$\gamma - mes$" events while the events of the second type as the "$\gamma - brem$" ones. A more detailed information about fundamental QCD subprocesses from which originate "$\gamma - mes$" and "$\gamma - brem$" events is presented in section 3.

The background may be also caused by "$e^{\pm}$ events" which contain one jet and $e^{\pm}$ as a direct photon candidate. The value of the fraction of these events in the total background was estimated in [31, 32] (see also sections 3, 4).

The background containing the "γ–mes" events can be significantly suppressed by the event selection criteria, pointed in [31, 32, 34]. It may be achieved, first of all, due to very strict photon isolation criteria because a parent meson (π^0, η, ω or K_s^0) is usually surrounded by other particles. Additional rejection factors were obtained from a full GEANT simulation of the physical processes in the CMS detector [40] where for the Barrel region ($|\eta| < 1.4$) we used an information from the electromagnetic calorimeter (ECAL) cells only [8] [42] while for the Endcap region ($1.4 < |\eta| < 2.5$) the results of the analysis of hits in the preshower detector [43] were applied.

An especial attention should be paid to the events containing the bremsstrahlung photons. They are also noticeably rejected by the selection cuts but still constitute a significant part of the total background [31, 32].

The simulation, performed with a help of the Monte Carlo event generator PYTHIA [44], has shown that in the selected "$\gamma + jet$" event samples the most part of "$\gamma - brem$" events contain a gluon jet (see section 4). For this part of events, as well as for a part of "$\gamma - mes$" events with a gluon jet, one can take into consideration the quark/gluon separation efficiencies found earlier in [45] [9]. The number of remained background events also must be well estimated in order to separate their contribution from one of the "$\gamma^{dir} + jet$" events (2).

3. Definition of selection cuts [10]

1. We shall select the events with one jet and one "γ^{dir}-candidate" (in what follows we shall denote it also as $\tilde{\gamma}$ and call the "photon" for brevity) with

$$P_t{}^{jet} \geq 30\ GeV/c \quad \text{and} \quad P_t{}^{\tilde{\gamma}} \geq 40\ GeV/c\,. \tag{7}$$

In our simulation the signal (most energetic γ or $e^{\pm}$ together with surrounding particles) is considered as a candidate for a direct photon if it fits into one CMS calorimeter

[8] A preshower detector is not foreseen currently in the Barrel region of the CMS detector [40].

[9] see also [46, 47].

[10] In this section we follow mostly the selection criteria from [31, 34].

tower having the size of 0.087×0.087 in the $\eta - \phi$ space [40].

For our applications a jet is defined according to the PYTHIA jetfinding algorithm LUCELL [44]. In the $\eta - \phi$ space the jet cone of radius R counted from the jet initiator cell is taken to be $R=((\Delta\eta)^2 + (\Delta\phi)^2)^{1/2} = 0.7$.

2. To suppress the contribution of background processes, i.e. to select mostly the events with the "isolated" photons and to discard the events that fake a direct photon signal, we restrict:

a) the value of the scalar sum of P_t of hadrons and other particles surrounding a photon within a cone of $R^{\gamma}_{isol} = ((\Delta\eta)^2 + (\Delta\phi)^2)^{1/2} = 0.7$ ("absolute isolation cut")

$$\sum_{i \in R_{isol}} P_t{}^i \equiv P_t{}^{isol} \leq P_{tCUT}^{isol}; \tag{8}$$

b) the value of a fraction ("fractional isolation cut")

$$\sum_{i \in R_{isol}} P_t{}^i / P_t{}^{\tilde{\gamma}} \equiv \epsilon^{\gamma} \leq \epsilon^{\gamma}_{CUT}; \tag{9}$$

3. We accept only the events having no charged tracks[11] with $P_t > 1\ GeV/c$ contained inside the cone of $R = 0.4$ around a γ^{dir}-candidate.

4. To suppress the background events with photons resulting from π^0, η, ω and K^0_S meson decays, we require the absence of a high P_t hadron in the tower containing the γ^{dir}-candidate:

$$P_t{}^{hadr} \leq 7\ GeV/c. \tag{10}$$

At the PYTHIA level of simulation this cut may effectively takes into account the imposing of an upper cut on the HCAL energy in the cells behind the ECAL signal cells fired by the direct photon. In real experimental conditions one can require for a fraction of the photon energy, deposited in ECAL to be greater than some threshold[12].

5. We select the events with the vector $\vec{P}_t{}^{jet}$ being "back-to-back" to the vector $\vec{P}_t{}^{\tilde{\gamma}}$ (in the plane transverse to the beam line) within $\Delta\phi$ defined by the equation:

$$\phi_{(\gamma,jet)} = 180^{\circ} \pm \Delta\phi, \tag{11}$$

where the angle $\phi_{(\gamma,jet)}$ between vectors $\vec{P}_t{}^{\tilde{\gamma}}$ and $\vec{P}_t{}^{jet}$ is calculated from $\vec{P}_t{}^{\tilde{\gamma}} \vec{P}_t{}^{jet} = P_t{}^{\tilde{\gamma}} P_t{}^{jet} cos(\phi_{(\gamma,jet)})$ with $P_t{}^{\tilde{\gamma}} = |\vec{P}_t{}^{\tilde{\gamma}}|$ and $P_t{}^{jet} = |\vec{P}_t{}^{jet}|$. The value of $\Delta\phi$ may be chosen from the interval $5^{\circ} \div 15^{\circ}$ for various energies.

6. We choose the events that do not have any other, except one jet, minijet (or cluster) high P_t activity with the $P_t{}^{clust}$ higher than some threshold P_{tCUT}^{clust} value. Thus we select events with

[11] i.e. particles as we use the PYTHIA level of simulation.

[12] e.g. to be greater than 0.95 (as it was used at D0 [7]).

$$P_t^{clust} \leq P_{tCUT}^{clust}, \tag{12}$$

where clusters are found by the same jetfinder LUCELL used to determine the main jet in the event. The most effective restrictions are $P_{tCUT}^{clust} = 5 \div 15\ GeV/c$. Their choice will be caused mostly by the gained statistics and $P_t^{\tilde{\gamma}}$ value (for higher $P_t^{\tilde{\gamma}}$ a weaker P_{tCUT}^{clust} can be used).

7. The events containing $e^{\pm}$ as a photon candidate are mainly caused by the following two subprocesses $q\,g \to q' + W^{\pm}$ and $q\,\bar{q}' \to g + W^{\pm}$ with the subsequent decay $W^{\pm} \to e^{\pm}\nu$. To reduce a contribution from these events [31, 32] we shall select only events having a small value of missing transverse momentum P_t^{miss}. So, we also use the following cut:

$$P_t^{miss} \leq P_{tCUT}^{miss}. \tag{13}$$

Finally, in what follows we shall set the values of the cut parameters (besides those pointed above explicitly) as specified below:

$$P_{tCUT}^{isol} = 2\ GeV/c,\ \ \epsilon_{CUT}^{\gamma} = 5\%,\ \ \Delta\phi \leq 15^{\circ},$$
$$P_{tCUT}^{clust} = 10\ GeV/c,\ \ P_{tCUT}^{miss} = 10\ GeV/c. \tag{14}$$

4. Determining the numbers of events and reducing the background

To estimate a background to the signal events we have done a simulation based on the Monte Carlo event generator PYTHIA 6.1 with a mixture of all existing in PYTHIA QCD and SM (including (3) and (4) [13]) subprocesses with large cross sections [14]. The total cross section of the background subprocesses exceeds the cross section of the subprocesses (3) and (4) by more than 3 orders of magnitude. The GRV 94L parameterization of the parton distribution functions is used as a default one.

Five generations (each of about 60–90 million events) with different values of minimal transverse momentum of a hard subprocess [15] $\hat{p}_{\perp}^{min}$ were done: $\hat{p}_{\perp}^{min}$ = 40, 70, 100, 140 and 200 GeV/c. The cross sections of the abovementioned subprocesses define the rates of corresponding physical events and, thus, appear here as weight factors. The selection criteria of section 2 were applied then to the generated events.

The total numbers of these events, i.e. events originated from subprocesses (3) and (4) as well as "$\gamma - brem$" and "$\gamma - mes$" events, are presented (being divided by the factor of 10^3) in Table 1 for each x and Q^2 interval ($Q^2 = (P_t^{\gamma})^2$) for the integrated luminosity [16] $L_{int} = 10\ fb^{-1}$. The momentum fractions x_a and x_b of the

[13] They have ISUB=14 and 29 according to the process numbers in PYTHIA [44].

[14] Namely, with ISUB=11–20, 28–31, 53, 68.

[15] CKIN(3) parameter in PYTHIA.

[16] This value is intended to be accumulated during one year of LHC running at luminosity $L = 10^{33}\ cm^{-2}s^{-1}$.

initial state partons were calculated via the photon and jet parameters according to formula (6) [11, 12]. The right-hand columns of this table shows, for a convenience, the correspondence of Q^2 interval to the P_t^{γ} interval.

One can see from Table 1 that at $40 < P_t^{\gamma} < 50\ GeV/c$ the total number of events is about 10 million and it drops to 24 200 at $200 < P_t^{\gamma} < 283\ GeV/c$, i.e. with five-fold increase of P_t^{γ} the spectrum drops about 400 times.

The contribution from the background "$e^{\pm}$ events" was not included in Table 1. The number of these type events was estimated in our previous papers [31, 32][17] and found to be very small as compared with other background types. Thus, in what follows we shall concentrate on more sizable background.

Now let us look at the contributions of different event types in different x and Q^2 intervals. The produced γ^{dir}-candidates were classified according to their origin, i.e. we consider separately those that are direct ones (i.e. produced in subprocesses (3) and (4)) and those that appear due to the radiation from quarks ("$\gamma - brem$" events) or from the π^0, η, ω and K_s^0 meson decays ("$\gamma - mes$" events). All these contributions are presented in Tables 1A–4A of Appendix (in a form of number of events divided by the factor of 10^3). .The numbers of events based on the Compton (3) and annihilation (4) subprocesses are shown in Tables 1A and 2A while the numbers of the "$\gamma - brem$" and "$\gamma - mes$" events can be found in Tables 3A and 4A, respectively[18]. These numbers were obtained after passing the selection criteria of section 2. The fractions of each event type, calculated for a given interval of P_t^{γ}, are presented in Fig. 1a (100% is taken for all types of events).

We see that the main part of the background is due to "$\gamma - brem$" events and the combined contribution of "$\gamma - brem$" and "$\gamma - mes$" events into the total number of events varies from about 23% at $40 < P_t^{\gamma} < 50\ GeV/c$ to about 6% at $100 < P_t^{\gamma} < 140\ GeV/c$ and drops to 4% at $200 < P_t^{\gamma} < 283\ GeV/c$.

We would like to stress that the essential point of our analysis is the study of the background contributions after application of the cuts for selecting the "$\gamma + jet$" events with (1) a limited cluster/minijet activity and (2) a clean $\gamma - jet$ topology[19]. Only in this case a contribution of both background types, "$\gamma - brem$" and "$\gamma - mes$" events, can be decreased noticeably[20].

[17] It was found that after the application of selection criteria from previous section and taking a track finding efficiency to be equal to 85% (being averaged over all pseudorapidity range) [41] a contribution of the $e^{\pm}$ events (having the isolated $e^{\pm}$ with $P_t^e > 40\ GeV/c$) to the total background reduces to less than 1% at $40 \leq P_t^e \leq 70\ GeV/c$ and to about 5% at $P_t^e \geq 100\ GeV/c$.

[18] See also [31, 32] for a more detailed information about background composition.

[19] See [31, 32] where the dynamics of application of the selection criteria is demonstrated.

[20] It was shown in [31, 32] that, for instance, at $P_t^{\gamma} > 100\ GeV/c$, the application of "photonic" cuts, usually used to select inclusive photon "$\gamma + X$" events, gives $S/B = 1.9$ only, while a further account of "hadronic" and topological cuts for selection of "$\gamma + jet$" events leads to $S/B = 17.6$, i.e *to the increase of S/B by about one order of magnitude* (here S is a total contribution from the events based on

Table 1: Numbers of all events (divided by 10^3) in Q^2 and x intervals for $L_{int} = 10\ fb^{-1}$.

Q^2	x values of a parton				All x	$P_t{}^{\gamma}$
$(GeV/c)^2$	10^{-4}–10^{-3}	10^{-3}–10^{-2}	10^{-2}– 10^{-1}	10^{-1}–10^{0}	10^{-4}–10^{0}	(GeV/c)
1600-2500	1393.6	4301.1	4506.8	481.4	10682.9	40–50
2500-5000	561.1	2931.0	3174.7	430.4	7097.2	50–71
5000-10000	61.7	665.6	769.6	196.1	1693.0	71–100
10000-20000	3.6	150.3	178.4	81.7	414.0	100–141
20000-40000	0.0	29.9	40.9	25.2	96.0	141–200
40000-80000	0.0	5.7	10.7	7.8	24.2	200–283
					20 007.3	

Table 2: Numbers of all events (divided by 10^3) in Q^2 and x intervals for $L_{int} = 10\ fb^{-1}$. $\epsilon^{\gamma/mes}$ separation efficiencies are taken into account.

Q^2	x values of a parton				All x	$P_t{}^{\gamma}$
$(GeV/c)^2$	10^{-4}–10^{-3}	10^{-3}–10^{-2}	10^{-2}– 10^{-1}	10^{-1}–10^{0}	10^{-4}–10^{0}	(GeV/c)
1600-2500	1214.6	3073.1	3433.1	394.5	8115.4	40–50
2500-5000	502.8	2220.7	2478.2	364.0	5565.8	50–71
5000-10000	54.1	532.8	587.8	168.7	1343.7	71–100
10000-20000	3.2	124.4	134.6	70.6	333.1	100–141
20000-40000	0.0	25.3	30.1	21.8	77.3	141–200
40000-80000	0.0	4.9	7.9	6.6	19.4	200–283
					15 454.7	

The selection criteria of section 2 are not final and are moderate enough. The results of their application may change if we shall vary some cuts. So, for example, a stronger limitation of cluster activity (12) by $P_{tCUT}^{clust} = 5\ GeV/c$ would lead to a further substantial decreasing of the numbers of "$\gamma - brem$" and "$\gamma - mes$" events [31, 32].

The contribution of "$\gamma - mes$" events can be also reduced by the account of the difference between a single photon and the π^0, η, ω and K_s^0 meson signals produced in the detector.

To take into account the discrimination efficiencies between a single photon and the photons produced via multiphoton decays of π^0, η, ω and K_s^0 mesons ($\epsilon^{\gamma/mes}$), we used the results of papers [42] and [43]. The efficiencies found in [42] were obtained by the analysis of the ECAL crystal cells only in the Barrel region ($|\eta| < 1.4$) while the efficiencies in [43] are found from the analysis of hits in the preshower detector in the Endcap region ($1.4 < |\eta| < 2.5$). The results of [42] and [43] are briefly the

the subprocesses (3) and (4) and B is a contribution from the sum of "$\gamma - brem$" and "$\gamma - mes$" events). The application of other cuts that limit a P_t activity out of the "$\gamma + jet$" system may lead to the following $20 - 30\%$ increase of the S/B ratio [31, 32].

following: the rejection efficiency of the neutral pion is about $49-67\%$ (depending on an energy) in the Barrel region and it ranges as $45-71\%$ for the Endcap region. The photon selection efficiencies (ϵ^{γ}_{sel}) were set to 70% and 91% in the first and second cases respectively [21].

The results of applications of the described above γ/meson separation efficiencies to the "$\gamma - mes$" events themselves are placed in Table 8A (compare with Table 4A) and in Tables 5A–7A of Appendix for other event types. Thus, we see that for the "$\gamma - mes$" events the reduction factor of about $2-3$ for $40 < P_t^{\tilde{\gamma}} < 100\ GeV/c$ can be obtained with a loss of $16-19\%$ of events of other types with a single photon in the final state. The total numbers of all events left after account of the $\epsilon^{\gamma/mes}$ separation efficiencies are shown in Table 2.

The physical models implemented in PYTHIA allows to get an idea about a possible origination of the "$\gamma - brem$" and "$\gamma - mes$" events. Tables 3 and 4 show the relative contributions of four main (having the largest cross sections) fundamental QCD subprocesses $qg \to qg$, $qq \to qq$, $gg \to q\bar{q}$ and $gg \to gg$ into a production of the "$\gamma - brem$" and "$\gamma - mes$" events selected with the criteria 1–7 of section 2 for three $P_t^{\tilde{\gamma}}$ intervals [22]. One can see from these tables that most of "$\gamma - brem$" and "$\gamma - mes$" events (from 70 to 80%) still originate from "gluonic" $qg \to qg$, $gg \to q\bar{q}$ and $gg \to gg$ subprocesses with dominant contribution from the first subprocess.

The analysis of the PYTHIA simulation output also shows that practically in all of selected "$\gamma - brem$" events the "bremsstrahlung photons" are produced in the final state of the fundamental subprocess. They are radiated from the outgoing quarks in the case of the first three subprocesses or can appear as the result of string breaking in the case of $gg \to gg$ scattering. The last mechanism, naturally, gives a small contribution into the "$\gamma - brem$" events production. In the first case the selected (see section 3) photon carries away almost all energy of a quark in the final state. The events of this kind have mostly a gluon jet (70.6% of events for $40 < P_t^{\tilde{\gamma}} < 71\ GeV/c$ interval and 58.7% of events for $141 < P_t^{\tilde{\gamma}} < 283\ GeV/c$) with the photon radiated in back-to-back direction to the jet in ϕ plane. In the second case ($gg \to gg$ based events) a remained jet is practically always of the gluon type.

As for "$\gamma - mes$" events, it is naturally to expect that in the events based on the $qg \to qg$ scattering after suppression of the cluster activity by the cut $P_t^{clust} <$

[21] With the same $\epsilon^{\gamma}_{sel} = 70\%$ one can reject about $90-95\%$ of "$\eta-$meson events" and $55-92\%$ of "K^0_s-meson events" [42] in the Barrel region. For the Endcap the respective rejection efficiencies were taken here equal to those obtained for π^0 meson. At the same time it is worth to note that the main contribution to the "$\gamma - mes$" background comes from the "π^0-events" ($\sim 62-65\%$ in the interval $40 < P_t^{\tilde{\gamma}} < 140\ GeV/c$).

[22] The sum over contributions from the four considered QCD subprocesses in some lines of Tables 3 and 4 is less than 100%. The remained percentages correspond to other subprocesses (like $q\bar{q} \to q\bar{q}$ or $qg \to q'W^{\pm}$). The errors in those tables are statistical and caused by the number of entries for various background types after application of the criteria 1–7 of section 2.

Table 3: Relative contribution (in per cents) of main QCD subprocesses into the "$\gamma - brem$" events production.

$P_t^{\tilde{\gamma}}$	fundamental QCD subprocess			
(GeV/c)	$qg \to qg$	$qq \to qq$	$gg \to q\bar{q}$	$gg \to gg$
40–71	70.6± 8.7	21.1± 3.8	5.1± 1.6	2.6± 1.0
71–141	67.5± 7.3	23.6± 3.5	4.2± 1.2	2.6± 0.9
141–283	58.7± 9.0	30.7± 5.7	1.8± 1.0	—

Table 4: Relative contribution (in per cents) of main QCD subprocesses into the "$\gamma - mes$" events production.

$P_t^{\tilde{\gamma}}$	fundamental QCD subprocess			
(GeV/c)	$qg \to qg$	$qq \to qq$	$gg \to q\bar{q}$	$gg \to gg$
40–71	65.2± 9.9	20.1± 4.5	7.1± 2.5	7.2± 2.3
71–141	63.7±11.6	23.0± 5.2	7.2± 2.6	4.4± 1.4
141–283	57.7±26.2	23.1±13.9	7.7± 6.9	3.8± 4.6

10 GeV/c (see (12)) a remained jet can originate with an equal probability from a quark as well as from a gluon (50% by 50%) while in the events based on the $qq \to qq$, $gg \to q\bar{q}$ ($gg \to gg$) subprocesses the jet is always of the quark (gluon) type.

Thus, one can conclude that about 73% (40%), 70% (36%) and 59% (33%) of the "$\gamma - brem$" ("$\gamma - mes$") events have a gluon jet in the selected one-jet events at $P_t^{\tilde{\gamma}}$ intervals $40 - 71$, $71 - 141$ and $141 - 283$ GeV/c, respectively.

So, for the following suppression of the contributions from "$\gamma - brem$" and "$\gamma - mes$" events having a gluon jet in the final state one can apply the quark/gluon separation efficiencies ($\epsilon^{q/g}$) obtained earlier in [45]. After the full event simulations using the CMSJET package [**?**] and the analysis based on the neural network technique it was found in [45] that with account of the quark jet selection efficiency of about $65 - 67\%$ it is possible to reject $73 - 81\%$ of gluons jets [23] for P_t^{jet} varying from 40 to 200 GeV/c.

The numbers of different types of events after an account of the both $\tilde{\epsilon}^{\gamma/mes}$ and $\epsilon^{q/g}$ separation efficiencies

are presented in Tables 9A–12A of Appendix while their fractions (in %) are shown in Fig. 1c.

By comparing Tables 7A and 11A we can see that the numbers of "$\gamma - brem$" events [24] are reduced in $2.5 - 3$ times at the cost of the 35% loss of the events based on the subprocess (3) and their fraction from the total number of events become about

[23] This efficiency slightly depends on the jet transverse momentum P_t^{jet} and pseudorapidity η^{jet} [45].

[24] that are, in fact, irreducible by using only photon information after application of the strong isolation cuts (8) and (9).

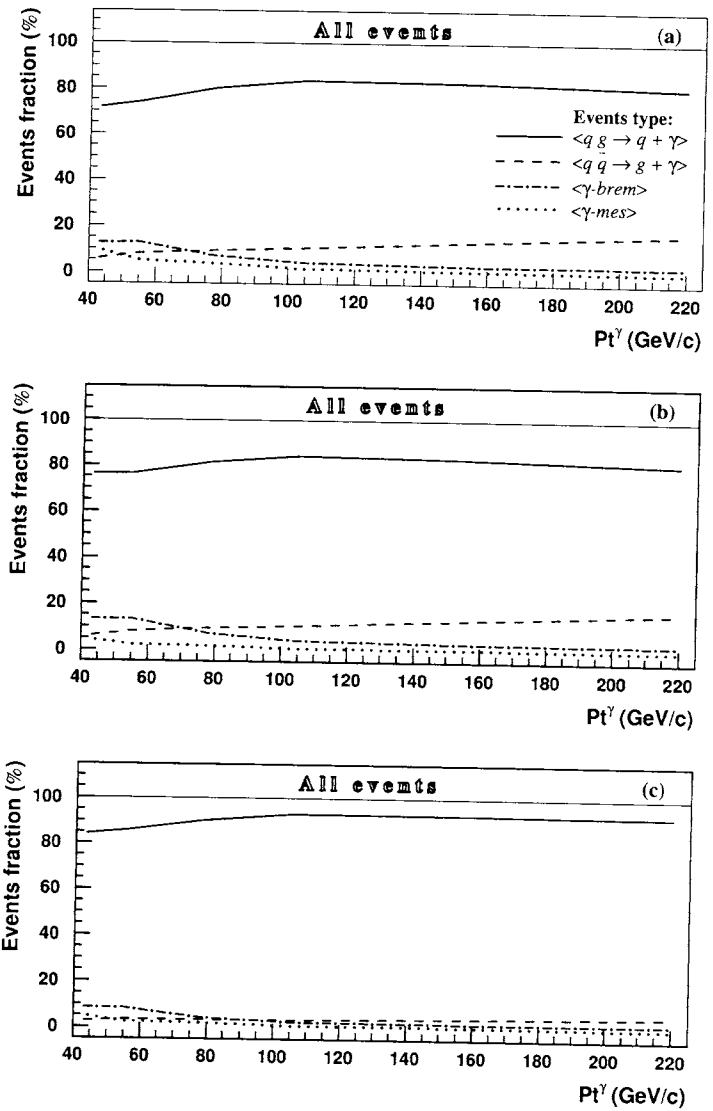

Fig. 1: The contributions of various events types to the total number of events as a function of P_t^{γ} presented for three cases: **(a)** No separation efficiency is taken into account, **(b)** $\epsilon^{\gamma/mes}$ separation efficiencies are taken into account and **(c)** $\epsilon^{\gamma/mes}$ and $\epsilon^{q/g}$ separation efficiencies are taken into account.

8% at $40 < P_t^{\tilde{\gamma}} < 50\ GeV/c$ and about 2% at $140 < P_t^{\tilde{\gamma}} < 200\ GeV/c$. *The total contributions of the "$\gamma-brem$" and "$\gamma-mes$" events in the same $P_t^{\tilde{\gamma}}$ intervals compose* 13.2% *and* 2.8%, *respectively.*

We see also that the account of $\epsilon^{q/g}$ separation efficiency reduces the contribution of events with annihilation subprocess (4) to the total number of events (especially at higher P_t^{γ}) to the size of about $3-5\%$ over all considered P_t^{γ} range (see Fig. 1 and Tables 1A–8A).

The final numbers of all "$\gamma + jet$" events for the luminosity $L_{int} = 10\ fb^{-1}$ at different x and Q^2 intervals after an account of the both separation efficiencies are given in Table 5. We see that after passing all selection cuts and application of the $\epsilon^{\gamma/mes}$ and $\epsilon^{q/g}$ efficiencies one can get about 5 million events at the $40 < P_t^{\tilde{\gamma}} < 50\ GeV/c$ interval, about 200 000 at $100 < P_t^{\tilde{\gamma}} < 141\ GeV/c$ and about 11 000 at the last considered interval $200 < P_t^{\tilde{\gamma}} < 283\ GeV/c$. *The total expected statistics on the "$\gamma + jet$" events, left after account of the $\epsilon^{\gamma/mes}$ and $\epsilon^{q/g}$ efficiencies, is about* $9 \cdot 10^6$ *events.* The final contributions of different subprocesses in various x and Q^2 intervals are presented in Tables 9A–12A.

Table 5: Numbers of all events (divided by 10^3) in Q^2 and x intervals for $L_{int} = 10\ fb^{-1}$. $\epsilon^{\gamma/mes}$ and $\epsilon^{q/g}$ separation efficiencies are taken into account.

Q^2	x values of a parton				All x	P_t^{γ}
$(GeV/c)^2$	10^{-4}–10^{-3}	10^{-3}–10^{-2}	10^{-2}– 10^{-1}	10^{-1}–10^{0}	10^{-4}–10^{0}	(GeV/c)
1600-2500	721.3	1858.7	2052.9	217.6	4850.5	40–50
2500-5000	302.3	1314.1	1449.4	206.2	3271.9	50–71
5000-10000	31.5	320.0	350.0	99.9	801.5	71–100
10000-20000	1.9	74.4	81.1	41.8	199.1	100–141
20000-40000	0.0	14.9	18.2	12.6	45.6	141–200
40000-80000	0.0	2.9	4.5	3.8	11.2	200–283
					9 179.8	

5. Conclusion

The results presented above show that during one year of the LHC running at low luminosity ($L = 10^{33}\ cm^{-2}s^{-1}$) one can collect after application of the proposed selection criteria (see [31, 34] and section 2 of this paper) the clean sample of "$\gamma^{dir} + jet$" events with a sufficient statistics to determine a gluon density in a proton in new kinematic region of $2 \cdot 10^{-4} \leq x \leq 1$ and $40 \leq P_t^{\tilde{\gamma}} \leq 280\ GeV/c$ (see Tables 1 and 1A–4A of Appendix).

After application of the selection cuts 1–7 of section 2 the combined contribution of the events with bremsstrahlung photons ("$\gamma - brem$") and the events with

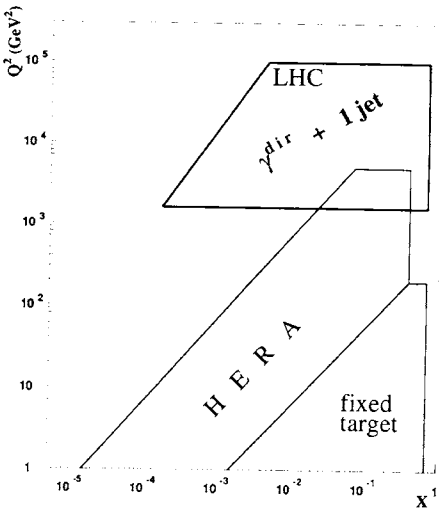

Fig. 2: LHC (x, Q^2) kinematic region for $pp \to \gamma + jet$ process.

photons resulting from high-energetic π^0, η, ω and K_s^0 meson decays ("$\gamma - mes$") is estimated to be about 23% at $40 < P_t^{\tilde{\gamma}} < 50\ GeV/c$ and it drops to 4% at $200 < P_t^{\tilde{\gamma}} < 283\ GeV/c$ (see also Tables 1A–4A and Fig. 1a).

The given estimations on contributions of the "$\gamma - brem$" and "$\gamma - mes$" events are yet not final. For instance, a stronger limitation $P_{tCUT}^{clust} = 5\ GeV/c$ (see (12)) would lead to a following substantial (about 30%) reduction of their contribution [31, 32].

With an additional account of discrimination efficiencies between single photons and π^0, η, K_s^0 mesons as well as those between quark and gluon jets (that were found in previous papers [42, 43, 45]) one can increase noticeably the purity of the selected samlples of the "$\gamma^{dir} + jet$" events (see Tables 9A–12A of Appendix and Fig. 1). A possibility to obtain better background rejection factors will depend on the chosen values of single photon and quark jet selection efficiencies[25] which are in their turn will be caused by a gained statistics of the "$\gamma + jet$" events.

It is also worth mentioning that a full simulation[26] of the signal and background processes is rather difficult due to a very small selection efficiency for the background

[25]Let us remind that the single photon selection efficiencies equal to 70% and 91% for the Barrel and Endcap regions and quark jet selection efficiencies equal to about 65% were chosen here for the given estimations.

[26]We mean a full simulation of the detector response with the following digitization and reconstruction of signals from physical objects.

events ($\approx 0.01 - 0.05\%$ depending on an energy) [31, 32] what, in its turn, requires huge computational resources to collect the background events statistics sufficient for the analysis.

Fig. 2 shows in the widely used (x, Q^2) kinematic plot (see also [48]) what area can be covered for studying the process $q\,g \to \gamma + q$. From this figure (and Tables 1, 2, 5) it becomes clear that even at low LHC luminosity it would be possible to study the gluon distribution with a good statistics of "$\gamma + jet$" events in the region of small x at values of Q^2 that are about 2 orders of magnitude higher than those reached at HERA now. It is worth emphasizing that an extension of experimentally reachable region at LHC to the region of lower values of Q^2, overlapping with the area covered by HERA, would be also of a big interest.

Appendix

Table 1A. Numbers of "$qg \to q + \gamma$" events (divided by 10^3) in Q^2 and x intervals at $L_{int} = 10\ fb^{-1}$.

Q^2	x values of a parton				All x
$(GeV/c)^2$	10^{-4}–10^{-3}	10^{-3}–10^{-2}	10^{-2}– 10^{-1}	10^{-1}–10^{0}	10^{-4}–10^{0}
1600-2500	1040.3	3128.7	3202.5	275.6	7647.1
2500-5000	451.2	2185.8	2326.8	280.8	5244.6
5000-10000	45.4	545.5	611.8	151.6	1354.4
10000-20000	2.9	125.5	151.1	66.7	346.2
20000-40000	0	24.6	35.2	19.9	79.6
40000-80000	0	4.7	8.5	6.2	19.4

Table 2A. Numbers of "$q\bar{q} \to \gamma + g$" events (divided by 10^3) in Q^2 and x intervals at $L_{int} = 10\ fb^{-1}$.

Q^2	x values of a parton				All x
$(GeV/c)^2$	10^{-4}–10^{-3}	10^{-3}–10^{-2}	10^{-2}– 10^{-1}	10^{-1}–10^{0}	10^{-4}–10^{0}
1600-2500	120.3	190.2	236.8	50.5	597.8
2500-5000	43.1	239.7	250.1	35.3	568.2
5000-10000	7.7	60.5	69.0	20.5	157.7
10000-20000	0.7	16.9	15.9	10.3	43.8
20000-40000	0	4.2	4.4	4.2	12.8
40000-80000	0	0.9	1.8	1.4	4.1

Table 3A. Numbers of "$\gamma - brem$" events (divided by 10^3) in Q^2 and x intervals at $L_{int} = 10\ fb^{-1}$.

Q^2	x values of a parton				All x
$(GeV/c)^2$	10^{-4}–10^{-3}	10^{-3}–10^{-2}	10^{-2}– 10^{-1}	10^{-1}–10^{0}	10^{-4}–10^{0}
1600-2500	143.6	508.5	578.3	104.8	1335.3
2500-5000	51.3	328.2	432.1	94.8	906.5
5000-10000	4.3	42.0	59.0	13.7	119.0
10000-20000	0	5.2	9.2	2.8	17.2
20000-40000	0	0.9	0.9	1.0	2.8
40000-80000	0	0.1	0.4	0.2	0.7

Table 4A. Numbers of "$\gamma - mes$" events (divided by 10^3) in Q^2 and x intervals at $L_{int} = 10\ fb^{-1}$.

Q^2	x values of a parton				All x
$(GeV/c)^2$	10^{-4}–10^{-3}	10^{-3}–10^{-2}	10^{-2}– 10^{-1}	10^{-1}–10^{0}	10^{-4}–10^{0}
1600-2500	89.3	473.6	489.1	50.5	1102.4
2500-5000	15.5	177.3	165.6	19.4	377.7
5000-10000	4.3	17.6	29.5	10.3	61.6
10000-20000	0	2.6	2.2	1.9	6.7
20000-40000	0	0.2	0.4	0.2	0.8
40000-80000	0	0	0.02	0.01	0.03

Table 5A. Numbers of "$qg \to q + \gamma$" events (divided by 10^3) in Q^2 and x intervals at $L_{int} = 10\ fb^{-1}$. $\epsilon^{\gamma/mes}$ separation efficiencies are taken into account.

Q^2	x values of a parton				All x
$(GeV/c)^2$	10^{-4}–10^{-3}	10^{-3}–10^{-2}	10^{-2}– 10^{-1}	10^{-1}–10^{0}	10^{-4}–10^{0}
1600-2500	945.0	2387.4	2608.6	246.7	6187.8
2500-5000	410.5	1723.1	1865.0	253.0	4251.7
5000-10000	41.3	443.2	475.5	134.6	1094.6
10000-20000	2.6	105.0	114.5	58.7	281.0
20000-40000	0	20.9	25.9	17.3	64.2
40000-80000	0	4.0	6.3	5.3	15.7

Table 6A. Numbers of "$q\bar{q} \to \gamma + g$" events (divided by 10^3) in Q^2 and x intervals at $L_{int} = 10\ fb^{-1}$. $\epsilon^{\gamma/mes}$ separation efficiencies are taken into account.

Q^2	x values of a parton				All x
$(GeV/c)^2$	10^{-4}–10^{-3}	10^{-3}–10^{-2}	10^{-2}– 10^{-1}	10^{-1}–10^{0}	10^{-4}–10^{0}
1600-2500	109.5	142.9	192.6	451.0	490.2
2500-5000	39.2	185.1	196.8	29.7	451.0
5000-10000	7.0	48.7	54.1	17.9	127.8
10000-20000	0.6	13.8	12.1	8.8	35.4
20000-40000	0	3.5	3.2	3.5	10.2
40000-80000	0	0.7	1.3	1.1	3.2

Table 7A. Numbers of "$\gamma - brem$" events (divided by 10^3) in Q^2 and x intervals at $L_{int} = 10\ fb^{-1}$. $\epsilon^{\gamma/mes}$ separation efficiencies are taken into account.

Q^2	x values of a parton				All x
$(GeV/c)^2$	10^{-4}–10^{-3}	10^{-3}–10^{-2}	10^{-2}– 10^{-1}	10^{-1}–10^{0}	10^{-4}–10^{0}
1600-2500	129.9	394.3	476.6	87.2	1088.0
2500-5000	46.7	258.5	359.8	74.8	739.8
5000-10000	3.9	34.0	47.1	11.7	96.6
10000-20000	0	4.4	7.1	2.4	13.9
20000-40000	0	0.8	0.7	0.9	2.4
40000-80000	0	0.1	0.3	0.2	0.6

Table 8A. Numbers of "$\gamma - mes$" events (divided by 10^3) in Q^2 and x intervals at $L_{int} = 10\ fb^{-1}$. $\epsilon^{\gamma/mes}$ separation efficiencies are taken into account.

Q^2	x values of a parton				All x
$(GeV/c)^2$	10^{-4}–10^{-3}	10^{-3}–10^{-2}	10^{-2}– 10^{-1}	10^{-1}–10^{0}	10^{-4}–10^{0}
1600-2500	30.2	148.5	155.2	15.4	349.4
2500-5000	6.4	53.9	56.6	6.4	123.3
5000-10000	1.9	6.9	11.2	4.6	24.6
10000-20000	0	1.1	0.9	0.8	2.8
20000-40000	0	0.1	0.3	0.1	0.5
40000-80000	0	0	0.01	0.01	0.02

Table 9A. Numbers of "$qg \to q + \gamma$" events (divided by 10^3) in Q^2 and x intervals at $L_{int} = 10\ fb^{-1}$. $\epsilon^{\gamma/mes}$ and $\epsilon^{q/g}$ separation efficiencies are taken into account.

Q^2	x values of a parton				All x
$(GeV/c)^2$	10^{-4}–10^{-3}	10^{-3}–10^{-2}	10^{-2}– 10^{-1}	10^{-1}–10^{0}	10^{-4}–10^{0}
1600-2500	623.7	1575.7	1721.7	162.8	4084.0
2500-5000	271.0	1137.3	1230.9	167.0	2806.2
5000-10000	27.3	292.5	313.8	88.9	722.5
10000-20000	1.7	69.4	75.6	38.7	185.5
20000-40000	0.0	13.8	17.1	11.5	42.4
40000-80000	0.0	2.7	4.2	3.5	10.4

Table 10A. Numbers of "$q\bar{q} \to \gamma + g$" events (divided by 10^3) in Q^2 and x intervals at $L_{int} = 10\ fb^{-1}$. $\epsilon^{\gamma/mes}$ and $\epsilon^{q/g}$ separation efficiencies are taken into account.

Q^2	x values of a parton				All x
$(GeV/c)^2$	10^{-4}–10^{-3}	10^{-3}–10^{-2}	10^{-2}– 10^{-1}	10^{-1}–10^{0}	10^{-4}–10^{0}
1600-2500	29.1	37.8	51.0	12.0	129.9
2500-5000	9.9	46.2	48.9	7.5	112.4
5000-10000	1.5	10.7	11.9	3.9	27.9
10000-20000	0.1	2.6	2.3	1.7	6.7
20000-40000	0.0	0.7	0.6	0.7	1.9
40000-80000	0.0	0.1	0.2	0.2	0.6

Table 11A. Numbers of "$\gamma - brem$" events (divided by 10^3) in Q^2 and x intervals at $L_{int} = 10\ fb^{-1}$. $\epsilon^{\gamma/mes}$ and $\epsilon^{q/g}$ separation efficiencies are taken into account.

Q^2	x values of a parton				All x
$(GeV/c)^2$	10^{-4}–10^{-3}	10^{-3}–10^{-2}	10^{-2}– 10^{-1}	10^{-1}–10^{0}	10^{-4}–10^{0}
1600-2500	48.5	147.1	177.8	32.5	406.0
2500-5000	17.2	95.0	132.2	27.5	272.0
5000-10000	1.4	12.2	17.0	4.2	34.8
10000-20000	0.0	1.6	2.6	0.9	5.1
20000-40000	0.0	0.3	0.3	0.3	0.9
40000-80000	0.0	0.0	0.1	0.1	0.2

Table 12A. Numbers of "$\gamma - mes$" events (divided by 10^3) in Q^2 and x intervals at $L_{int} = 10\ fb^{-1}$. $\epsilon^{\gamma/mes}$ and $\epsilon^{q/g}$ separation efficiencies are taken into account.

Q^2	x values of a parton				All x
$(GeV/c)^2$	10^{-4}–10^{-3}	10^{-3}–10^{-2}	10^{-2}– 10^{-1}	10^{-1}–10^{0}	10^{-4}–10^{0}
1600-2500	19.9	98.0	102.5	10.2	230.6
2500-5000	4.2	35.6	37.4	4.2	81.4
5000-10000	1.3	4.6	7.4	3.0	16.2
10000-20000	0.0	0.8	0.6	0.5	1.9
20000-40000	0.0	0.1	0.2	0.1	0.3
40000-80000	0.0	0.0	0.01	0.01	0.02

Acknowledgments

We are greatly thankful to D. Denegri who stimulated us to study the physics of "$\gamma + jet$" processes, permanent support and fruitful suggestions. It is a pleasure for us to express our recognition for helpful discussions to P. Aurenche, M. Dittmar, M. Fontannaz, J.Ph. Guillet, M.L. Mangano, E. Pilon, H. Rohringer, S. Tapprogge, H. Weerts and J. Womersley.

References

[1] D. Denegri *et al*, "Summary of the CMS Discovery Potential for the MSSM SUSY Higgses", CMS NOTE 2001/032; S. Abdullin *et al*, "Discovery potential for supersymmetry in CMS", J.Phys.**G28** (2002)469, hep-ph/9806366; R. Kinnunen, "Higgs physics at LHC", CMS conference report, CMS CR 2002/020.

[2] P. Aurenche *et al.* Proc. of "ECFA LHC Workshop", Aachen, Germany, 4-9 Oktob. 1990, edited by G. Jarlskog and D. Rein (CERN-Report No 90-10; Geneva, Switzerland 1990), Vol. **II**.

[3] UA1 Collaboration, C. Albajar *et al.*, Phys.Lett, **209B** (1998)385.

[4] UA2 Collaboration, R. Ansari *et al.*, Phys.Lett. **176B** (1986)239.

[5] CDF Collaboration. F. Abe *et al.*, Phys.Rev.Lett. **68** (1992)2734; F. Abe *et al.*, Phys.Rev. **D48** (1993)2998; F. Abe *et al.*, Phys.Rev.Lett. **73** (1994)2662.

[6] D0 Collaboration, F. Abachi *et al.*, Phys.Rev.Lett. **77** (1996)5011.

[7] D0 Collaboration, B. Abbott *et al.*, Phys.Rev.Lett. **84**(2000)2786;
D0 Collaboration, V. Abazov *et al.*, Phys.Rev.Lett. **87**(2001)251805.

[8] P. Aurenche, J. Lindfors, Nucl.Phys.**B168**(1980)296.

[9] P. Aurenche, A. Douiri, R. Baier, M. Fontannaz, D. Schiff, Phys.Lett.**B140**(1984)87.

[10] T. Ferbel and W.R. Molzon, Rev.Mod.Phys. **56** (1984)181.

[11] J.F. Owens, Rev.Mod.Phys. **59** (1987)465.

[12] E.N. Argyres, A.P. Contogouris, N. Mebarki and S. D.P. Vlassopulos, Phys.Rev. **D35**, (1987)1584.

[13] P. Aurenche, *et al.* Phys.Rev. **D39** (1989)3275.

[14] E.L. Berger and J. Qiu, Phys.Rev. **D44** (1991)2002.

[15] J. Huston *et al.*, Phys.Rev. **D51** (1995)6139.

[16] W. Vogelsang and A. Vogt, Nucl.Phys. **B453** (1995)334.

[17] W. Vogelsang and M. Whally, J.Phys. **G23** (1997)A1.

[18] J. Huston ATLAS Note ATL-Phys-99-008, CERN,1999.

[19] S. Frixione and W. Vogelsang, CERN-TH/99-247 hep-ph/9908387.

[20] E706 Collaboration, L. Apanasevich *et al.*, Phys.Rev.Lett. **81** (1997)2642.

[21] UA6 Collaboration, G. Ballocchi *et al.*, Phys.Lett. **B436** (1998)222.

[22] A.D. Martin *et al.*, Eur.Phys.J. **C4** (1998)463.

[23] CTEQ Collaboration, H.L. Lai *et al.*, Eur.Phys.J. **C12** (2000)375.; see also http://www.phys.psu.edu/ cteq.

[24] P. Aurenche, M. Fontannaz, S. Frixione, Proc. of "CERN Workshop on Standard Model Physics (and more) at the LHC", QCD (section 6.1) "General features of photon production", Yellow Report CERN-2000-004, 9 May 2000, CERN, Geneva.

[25] ISR–AFS Collaboration, T. Akesson *et al.*, Zeit.Phys. **C34** (1987)293.

[26] UA2 Collaboration, J. Alitti *et al*, Phys.Lett, **B299** (1993)174.

[27] CDF Collaboration, F. Abe *et al.*,Phys.Rev. **D57** (1998)1359 (see also p.67).

[28] D.V. Bandourin, V.F. Konoplyanikov, N.B. Skachkov, "On the application of "$\gamma + jet$" events for setting the absolute jet energy scale and determining the gluon distribution at the LHC.", hep-ex/0207028.

[29] D.V. Bandourin, V.F. Konoplyanikov, N.B. Skachkov, "Events rate estimation for gluon distribution determination at LHC", hep-ex/0207028. Proc. of the XV ISHEP "Relativistic Nuclear Physics and Quantum Chromodynamics", Eds. A.M. Baldin, V.V. Burov, A.I. Malakhov. Dubna, 2001, v.I, pp.375-383.

[30] D.V. Bandourin, N.B. Skachkov, "On the possibilities of measuring gluon distribution in "gamma/Z0+jet" events at Tevatron Run II and LHC energies", Contributed to Proc. of XI International Workshop on Deep Inelastic Scattering, St. Petersburg, 2003.

[31] D.V. Bandourin, V.F. Konoplyanikov, N.B. Skachkov, "Jet energy scale setting with "$\gamma + jet$" events at LHC energies. Detailed study of the background suppression." JINR preprint E2-2000-255, hep-ex/0011017.

[32] D.V. Bandurin, V.F. Konoplyanikov, N.B. Skachkov. Setting the absolute scale for jet energy at CMS with $pp \to jet + \gamma + X$ events. Study of background suppression (To appear as CMS Note).

[33] M. Dittmar, F. Pauss, D. Zurcher, Phys.Rev. **D56** (1997)7284.

[34] D.V. Bandourin, V.F. Konoplyanikov, N.B. Skachkov, "Jet energy scale setting with "$\gamma + jet$" events at LHC energies. Generalities, selection rules." JINR preprint E2-2000-251, hep-ex/0011012.

[35] D.V. Bandourin, V.F. Konoplyanikov, N.B. Skachkov, "$\gamma + jet$" events rate estimation for gluon distribution determination at LHC", Part.Nucl.Lett. **103**(2000)34, hep-ex/0011015.

[36] M. Dittmar, K. Mazumdar, N. Skachkov, Proc. of "CERN Workshop on Standard Model Physics (and more) at the LHC", QCD (section 2.7), "Measuring parton luminosities and parton distribution functions", Yellow Report CERN-2000-004, 9 May 2000, CERN, Geneva.

[37] D.V. Bandurin, N.B. Skachkov. " "$\gamma + jet$" process application for setting the absolute scale of jet energy and determining the gluon distribution at the Tevatron Run II." D0 Note 3948, 2002, hep-ex/0203003.

[38] D.V. Bandourin, N.B. Skachkov, "Photon+jet event rate estimation for gluon distribution determination at the Tevatron RUN II", Contributed to Proc. of XVI ISHEP "Relativistic Nuclear Physics and Quantum Chromodynamics", Dubna, 2002. JINR Preprint E2-2002-154, hep-ex/0206040, *To appear in Yad.Fiz.*

[39] D.V. Bandourin, V.F. Konoplyanikov, N.B. Skachkov, "On the possibility of discrimination between $\pi^0, \eta, \omega, K_s^0$ mesons and a photon based on the calorimeter information in the CMS detector", JINR Communication E1-2001-261, hep-ex/0108050.

[40] CMS Electromagnetic Calorimeter Project, Technical Design Report, CERN/LHCC 97–33, CMS TDR 4, CERN, 1997.

[41] CMS Tracker Project, Technical Design Report, CERN/LHCC 98–6, CMS TDR 5, CERN, 1999.

[42] D.V. Bandourin, N.B. Skachkov. "Separation of a signle photon and products of the π^0, η, K_s^0 mesons neutral decay channels in the CMS electromagnetic calorimeter using neural network", JINR Communication E2-2001-259, hep-ex/0108051.

[43] A. Kyriakis, D. Loukas, J. Mousa, D. Barney, CMS Note 1998/088, "Artificial neural net approach to $\gamma - \pi^0$ discrimination using CMS Endcap preshower".

[44] T. Sjostrand, Comp.Phys.Comm. **82** (1994)74. The version 6.131 of PYTHIA was used.

[45] D.V. Bandourin, N.B. Skachkov, "Separation of quark and gluon jets in the direct photon production processes at the LHC using the neural network approach",JINR Communication E2-2001-260, hep-ex/0109001.

[46] L. Lonnblad, C. Peterson and T. Rognvaldsson, "Finding gluon jets with a neural trigger", Phys.Rev.Lett, **65** (1990)1321.

[47] L. Lonnblad, C. Peterson and T. Rognvaldsson, "Using neural network to identify jets", Nucl.Phys., **B349** (1991)675.

[48] R. Ball, M. Dittmar, W.J. Stirling, Proc. of "CERN Workshop on Standard Model Physics (and more) at the LHC", QCD, (section 2) "Parton distribution functons", Yellow Report CERN-2000-004, CERN, 2000.

Received on August 14, 2003.

Бандурин Д. В., Скачков Н. Б. E2-2003-164

О возможности измерения глюонного распределения в протоне в событиях «фотон + струя» на LHC

Оценивается число событий «фотон + струя», которые могут быть использованы для определения глюонного распределения в протоне $f_g^p(x,Q^2)$ на LHC для разных интервалов по x и Q^2. Изучаются вклады различных источников фоновых событий. Для оценки окончательного вклада фоновых событий в разных интервалах по x и Q^2 учитываются эффективности разделения кварковых и глюонных струй, а также одиночных фотонов и продуктов нейтральных каналов распада π^0-, η-, ω- и K_s^0-мезонов. Для моделирования физических событий, используемых в анализе, применяется генератор событий PYTHIA.

Работа выполнена в Лаборатории ядерных проблем им. В. П. Джелепова ОИЯИ.

Препринт Объединенного института ядерных исследований. Дубна, 2003

Bandurin D. V., Skachkov N. B. E2-2003-164

On the Possibility of Measuring the Gluon Distribution in Proton with «γ + jet» Events at LHC

The numbers of the «γ + jet» events suitable for a determination of the gluon distribution function $f_g^p(x,Q^2)$ in a proton at the LHC for various intervals of x and Q^2 are estimated. The contributions of different background sources are studied. The values of discrimination powers between quark and gluon jets as well as between a single photon and the products of π^0, η, ω and K_s^0 mesons decaying through the neutral channels are applied to estimate the final contributions of different event types to the «γ + jet» production in various intervals of x and Q^2. The PYTHIA event generator was used for modeling physical events for this analysis.

The investigation has been performed at the Dzhelepov Laboratory of Nuclear Problems, JINR.

Preprint of the Joint Institute for Nuclear Research. Dubna, 2003

Корректор *Т. Е. Попеко*

Подписано в печать 16.12.2003.
Формат 60 × 90/16. Бумага офсетная. Печать офсетная.
Усл. печ. л. 1,43. Уч.-изд. л. 2,27. Тираж 415 экз. Заказ № 54219.

Издательский отдел Объединенного института ядерных исследований
141980, г. Дубна, Московская обл., ул. Жолио-Кюри, 6.
E-mail: publish@pds.jinr.ru
www.jinr.ru/publish/